

Spiral Wave Meandering in Models of Ventricular Tissue as an Antiarrhythmic Target

GP Kremmydas¹, AV Holden²

¹LUMC-KI, Argostoli, Greece

²University of Leeds, Leeds, UK

Abstract

We characterise the effects of ionic conductance and concentration changes on the meandering patterns and dynamics of re-entrant excitation in models of mammalian ventricular tissue. An increase in the spatial extent of spiral wave meander might lead to an increased likelihood of self-termination of the re-entrant excitation, since the probability of the spiral core meeting and annihilating at the in-excitabile tissue boundaries is increased. Thus, the spiral-wave meandering behaviour and dynamics provides a potential target for antiarrhythmic drugs.

1. Introduction

Ventricular re-entrant arrhythmias can lead to fibrillation and cardiac death. Experimental and theoretical evidence suggests that such arrhythmias can appear in the absence of anatomical obstacles and even in apparently healthy myocardium. The underlying mechanism of re-entrant arrhythmias is believed to be the establishment of spiral waves of excitation in ventricular muscle [1]. The existence of spiral wave solutions is a common feature in reaction-diffusion equations of excitable media and the ability to support spiral wave excitation has been experimentally verified for cardiac tissue. Many basic characteristics of re-entrant arrhythmias can be understood by using homogenous reaction-diffusion models of cardiac tissue with reaction kinetics based on detailed biophysical equations of cardiac cell excitation. This approach can serve as the first step towards the computational reconstruction of virtual tissue and organ models in which further idiosyncratic features of cardiac tissue as an excitable medium such as anisotropy and inhomogeneity are incorporated.

In this study we characterise the effects of ionic conductance and concentration changes on the meandering patterns and dynamics of re-entrant excitation in models of mammalian ventricular tissue. Two-dimensional reaction-diffusion systems with kinetics based on the Oxsoft Heart[®] single guinea-pig ventricle cell and a recent

version of the Luo-Rudy phase II biophysical equations are used as idealised virtual tissue tools. The effect of altering model parameters on the spatial extent of spiral wave meander is used to assess the effectiveness of pharmacological manipulation of the corresponding biophysical parameters in altering the likelihood of self-termination of re-entrant excitation. An increased extent of meander increases the probability of spiral wave core meeting and annihilating at the in-excitabile tissue boundaries. Therefore, spiral wave meandering behaviour and dynamics provides a potential target for antiarrhythmic drugs. Such detailed investigation of antiarrhythmic action on models of cardiac excitation provides a useful virtual tissue engineering tool for the initial evaluation of appropriate drug therapies.

2. Methods

A two dimensional isotropic and homogenous excitable medium describing cardiac excitation can be modelled by the reaction-diffusion system

$$\begin{aligned}\partial_t V &= -1/C \sum_{i=1}^m I_{\text{ion},i} + D \nabla^2 V \\ \partial_t u_j &= f_j(u_1, u_2, \dots, u_j, \dots, u_{n-1}, V) \quad (1) \\ & j = 1, 2, \dots, n-1\end{aligned}$$

where V is the membrane potential, C is the specific membrane capacitance, $I_{\text{ion},i} = g_i(u_1, u_2, \dots, u_{n-1}, V)$ the set of transmembrane ionic currents, D the diffusion coefficient, ∇^2 the Laplacian operator and u_j the gating variables and ionic concentrations of the given model.

The exact form of the equations (1) for the Oxsoft Heart[®] single guinea-pig ventricle cell (GPV) are provided in [2] while for the Luo-Rudy model (LRII) in [3, 4, 5]. The equations for LRII used here were extracted from the source code in C++ available from the web-site <http://www.cwru.edu/med/CBRTC/LRdOnline>.

For both models, spiral waves were initiated by a phase distribution method [2] in a 20mm × 20mm medium discretised with a space step of 100 μm using a standard

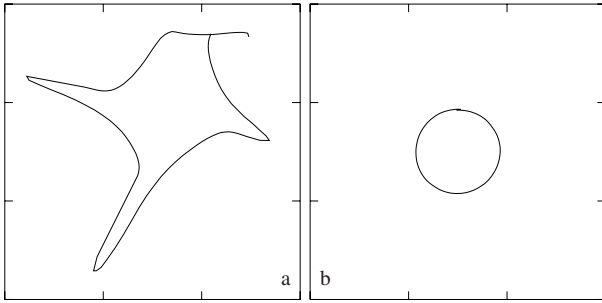


Figure 1. Tip trajectories for the GPV (a) and the LRII (b) model (size for both plots is $3\text{mm}\times 3\text{mm}$) defined as the intersection of the corresponding V isolines with the isoline of an appropriately selected gating variable (I_{Ca} gating variable $f=0.5$ for GPV and $I_{Ca,L}$ gating variable $f=0.4$ for LRII).

5-point discretisation for the Laplacian operator (see fig. 1) and non-flux boundary conditions. The equations (1) were integrated using a semi-explicit Euler method (gating variables were calculated implicitly at every time step) with $\Delta t = 10\mu\text{s}$ and $D=60\text{mm}^2/\text{s}$ for LRII and $\Delta t = 50\mu\text{s}$ and $D=31.25\text{mm}^2/\text{s}$ for GPV (the selected D values correspond to solitary plane wave propagation velocity of $\approx 0.4\text{m/s}$).

Spiral wave tip trajectories were defined as the intersection of $V=-10\text{mV}$ and $u_{GPV}=0.5$ isolines (u_{GPV} is a gating variable for I_{Ca}) for GPV and $V=-40\text{mV}$ and $u_{LRII}=0.4$ isolines (gating variable for the L-type calcium current $I_{Ca,L}$) for LRII.

Spiral-wave re-entrant activity in each model was simulated for 2s and for each simulation a transmembrane ionic conductance (g_{Na} , g_{Kr} , g_{Ks}), an extracellular ionic concentration ($[Na^+]_o$, $[Ca^{2+}]_o$, $[K^+]_o$) or the permeability of the cardiac cell membrane to Ca^{2+} ions P_{Ca} was altered and the spiral tip trajectory ($x_{tip}(t)$, $y_{tip}(t)$) was monitored on the (x, y) -plane. Among these parameters g_{Kr} and g_{Ks} are unique to LRII since GPV does not incorporate the corresponding ionic currents (I_{Kr} and I_{Ks}). The spatial extent of spiral wave meander was quantified as the minimum radius R_{meand} of a circle enclosing the tip trajectory over a whole period at the end of each simulation.

3. Results

Tip trajectories for spiral wave simulations with “standard” parameters for GPV and LRII are shown in figure 1. A characteristic five-lobe meandering pattern is apparent in the GPV model with $R_{meand}=1.14\text{mm}$ (1.a) while in the LRII model (1.b) the spiral wave rigidly rotates around a circular core ($R_{meand}=0.43\text{mm}$). Near the spiral wave tip, the curvature of the wavefront becomes

very close to its critical value and excitation propagation slows down.

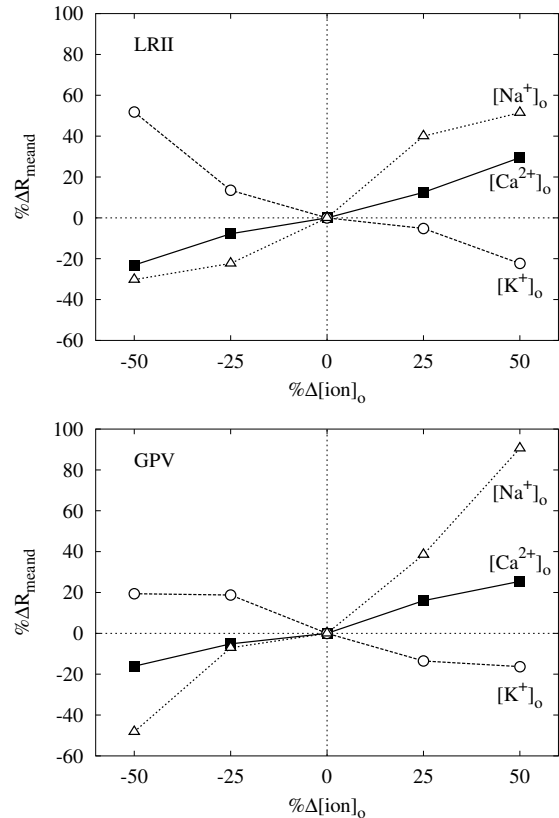


Figure 2. Effects of extracellular ion concentration changes on the spatial extent of spiral wave meandering in LRII (top) and GPV (bottom) model expressed as % change in R_{meand} versus % change in ion concentrations. Standard values ($0\% \Delta[\text{ion}]_o$) are for GPV: $[Na^+]_o=140\text{mM}$, $[Ca^{2+}]_o=2\text{mM}$, $[K^+]_o=4\text{mM}$ and for LRII: $[Na^+]_o=140\text{mM}$, $[Ca^{2+}]_o=1.8\text{mM}$, $[K^+]_o=4.5\text{mM}$.

Using the two idealised virtual-tissue models a set of *in silico* “experiments” were conducted to investigate the effects of parameter changes on the dynamics of spiral wave re-entry. Figure 2 summarizes the results of experiments investigating the effects of altering extracellular ionic concentrations on the spatial extent of spiral wave meandering. Per cent changes of meandering size ΔR_{meand} are plotted versus per cent change in the corresponding extracellular ionic concentrations. In both the GPV and LRII model increasing $[Na^+]_o$ and $[Ca^{2+}]_o$ led to an increase of meandering extent while the increase of $[K^+]_o$ had an opposite effect.

The sodium current I_{Na} activates during the rising phase of the action potential and its amplitude affects the maximum depolarisation rate (maximum dV/dt) and

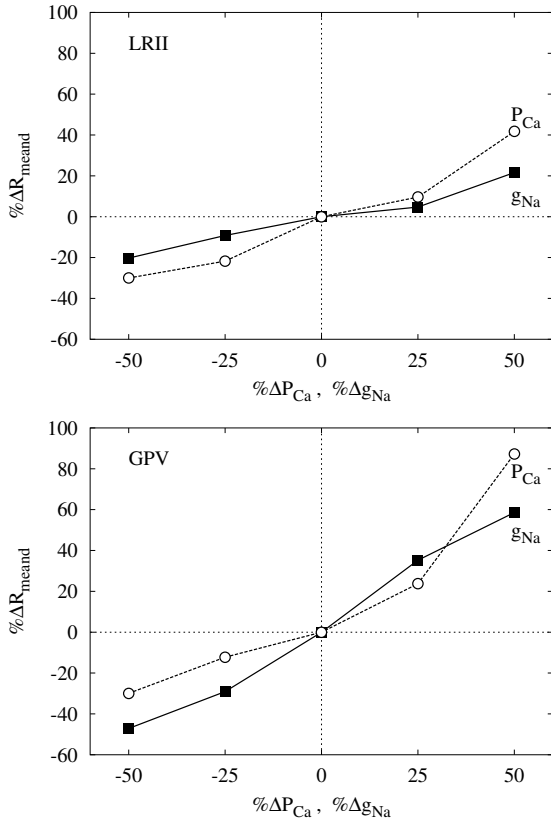


Figure 3. Effect of changes in sodium conductance g_{Na} and Ca^{2+} permeability P_{Ca} on spatial extent of meandering. Standard values are for LRII: $g_{Na}=16\text{mS}/\mu\text{F}$ $P_{Ca}=5.4\times 10^{-4}\text{cm/s}$ and GPV: $g_{Na}=2.5\mu\text{S}$, $P_{Ca}=0.25\text{nA/mM}$

thus the conduction velocity of activation wavefronts in cardiac tissue. Persistent inactivation of I_{Na} occurs inside the inexcitable spiral core around which spiral waves persistently rotate. Pathophysiological conditions or pharmacological interventions that alter the sodium conductance g_{Na} would significantly affect the dynamics of spiral wave reentry in cardiac muscle. Figure 3 summarises the results of numerical experiments on the effects of altering the fast sodium conductance (g_{Na}) and membrane permeability to Ca^{2+} ions (P_{Ca}). In LRII and GPV increasing g_{Na} and P_{Ca} extends the meander size of spiral waves. Our results are consistent with analogous simulations (see [6], figure 7) on the effects of g_{Na} changes on the spatial extent of meandering for different types of the long QT syndrome, using modifications of the GPV model in which the equations for I_{Kr} and I_{Ks} were added. It should be noted that our GPV model does not include the potassium currents incorporated in [6] which are also present in the LRII model presented here.

Another difference between the two models presented

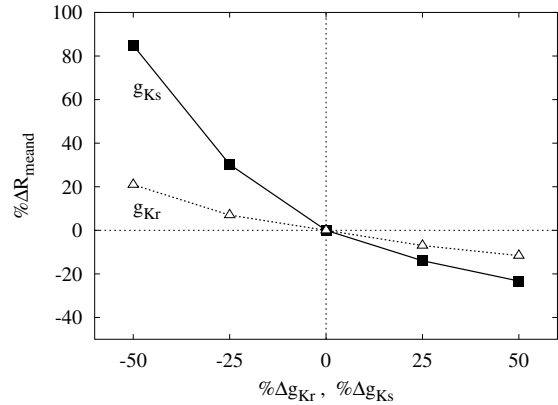


Figure 4. Effects of altering g_{Kr} and g_{Ks} on meander size in LRII.

here is that P_{Ca} is implicated in the equation for the Ca^{2+} -mediated slow inward current I_{Ca} of the GPV model while in the LRII model it affects the Ca^{2+} -mediated component of the L-type calcium current $I_{Ca,L}$. The L-type current together with the T-type (transient) calcium current $I_{Ca,T}$ have in more recent models replaced the older slow inward I_{Ca} current. This difference could explain the higher extent of meandering in GPV compared to LRII model for similar changes in P_{Ca} : in GPV the “bulk” I_{Ca} current is affected while in LRII only the calcium part of one of its components ($I_{Ca,L}$) is affected (the total $I_{Ca,L}$ current has also K^+ and Na^+ mediated components controlled by the corresponding ion permeability).

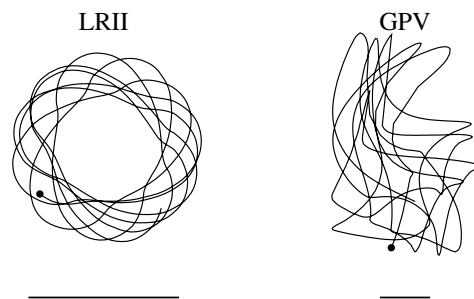


Figure 5. Meandering patterns for the LRII and GPV models. Tip trajectories (plotted in different spatial scale) correspond to 700ms of re-entrant activity in simulations in which P_{Ca} was increased by 50% with respect to the “standard” value of each model (cf. figure 3). The horizontal bars correspond to a length of 1mm.

The potassium mediated currents I_{Kr} and I_{Ks} are implicated in known clinical syndromes like certain types of the long QT syndrome and their role has been examined in virtual tissue studies [6, 7]. The results of numerical experiments on LRII model, summarised in figure 4, explore the effects of changes in g_{Kr} and g_{Ks}

conductances. Decreasing g_{Ks} (blocking I_{Ks}) corresponds to LQT1 syndrome while decreasing g_{Kr} (blocking I_{Kr}) corresponds to LQT2 syndrome.

In figure 5 examples of meandering patterns for each of the two models are shown. At certain parameter ranges the rigid spiral wave rotation observed at “standard” parameter values of the LRII model is replaced by essentially bi-periodic meandering patterns. Such transition from simple rigid rotation to more complex (and even chaotic) meandering patterns has also been observed and studied in excitable media with simple phenomenological reaction kinetics [8]. The GPV model is rich in meandering patterns [9] with a characteristic five-lobe meandering pattern at certain ranges of parameters (cf. figure 1). This five-lobe pattern is attributed to the interplay of I_{Na} and I_{Ca} near the spiral core [10] and can be abolished or altered into different patterns by changes in biophysical model parameters [9].

4. Discussion

Ventricular arrhythmias and fibrillation are potentially lethal conditions. Re-entrant propagation in the absence of anatomical obstacles has been demonstrated as a mechanism generating these conditions in computational and animal models [1]. Self-terminating ventricular arrhythmias have been observed in patients. One possible explanation for self-termination of spiral wave re-entry is by meandering to and annihilation at an inexcitable boundary. It has been proposed [6] that the spatial extent of meander of a re-entrant wave in the heart can be directly related to the probability of self-termination and thus inversely related to the lethality of the corresponding conditions of the myocardium (e.g. presence of a clinical syndrome affecting excitability parameters).

The virtual tissue experiments presented here indicate that the manipulation of biophysical parameters affecting cardiac excitability - by pharmacological or other interventions - can alter the probability of self-termination and therefore the lethality of re-entrant arrhythmias. This can be achieved through the changes in the spatial extent of meander brought about by such interventions. Recent advances in drug design and gene-therapy interventions make possible the specific manipulation of appropriate biophysical parameters and ion channel properties. In this direction, virtual tissues can be an indispensable exploratory tool for the routine testing of new therapeutic strategies.

Acknowledgements

We would like to thank Dr. V.N. Biktashev for comments and suggestions on the work presented here.

References

- [1] Gray RA, Jalife J. Spiral waves and the heart. *Int J Bifurc Chaos* 1996;6:415–435.
- [2] Biktashev VN, Holden AV. Re-entrant activity and its control in a model of mammalian ventricular tissue. *Proc Roy Soc Lond B* 1996;263:1373–1382.
- [3] Luo CH, Rudy Y. A dynamic model of the cardiac ventricular action potential. I. Simulations of ionic currents and concentration changes. *Circ Res* 1994;74(6):1071–1096.
- [4] Luo CH, Rudy Y. A dynamic model of the cardiac ventricular action potential. II. Afterdepolarizations, triggered activity, and potentiation. *Circ Res* 1994; 74(6):1097–1113.
- [5] Faber GM, Rudy Y. Action potential and contractility changes in $[Na^+]_i$ overloaded cardiac myocytes: a simulation study. *Biophys J* 2000;78(5):2392–2404.
- [6] Clayton RH, Bailey A, Biktashev VN, Holden AV. Re-entrant cardiac arrhythmias in computational models of long QT myocardium. *J Theor Biol* 2001;208(2):215–225.
- [7] Aslanidi OV, Bailey A, Biktashev VN, Clayton RH, Holden AV. Enhanced self-termination of re-entrant arrhythmias as a pharmacological strategy for antiarrhythmic action. *Chaos* 2002;12(3):843–851.
- [8] Zhang H, Holden AV. Chaotic meander of spiral waves in the FitzHugh-Nagumo system. *Chaos Solitons Fractals* 1995;5(3-4):661–670.
- [9] Kremmydas GP, Holden AV. Spiral-wave meandering in reaction-diffusion models of ventricular muscle. *Chaos Solitons Fractals* 2002;13(8):1659–1669.
- [10] Biktashev VN, Holden AV. Reentrant waves and their elimination in a model of mammalian ventricular tissue. *Chaos* 1998;8:48–56.

Address for correspondence:

George P. Kremmydas
Research, Technology & Development Dept.
LUMC-KI, Lithstroto 27, Argostoli
GR 28100, Kefalonia, GREECE
tel: ++30-2671-029050, fax: ++30-2671-029052
george@kefalonia-ithaki.gr